J. Appl. Comput. Mech., 6(SI) (2020) 1069-1083
DOI: 10.22055/JACM.2019.31964.1946

ISSN: 2383-4536
jacm.scu.ac.ir

Shahid Chamran University of Ahvaz

Journal of Applied and Computational Mechanics

Research Paper

Poiseuille Flow with Couple Stresses Effect and No-slip Boundary Conditions

Akil J. Harfash[1], **Ghazi A. Meften**[2]

[1] Department of Mathematics, College of Sciences, University of Basrah, Basrah, Iraq, Email: akilharfash@gmail.com,

[2] Department of Mathematics, College of Education for Pure Sciences, University of Basrah, Basrah, Iraq, Email: ghazialbazony@gmail.com

Received December 16 2019; Revised December 25 2019; Accepted for publication December 25 2019.
Corresponding author: A.J. Harfash (akilharfash@gmail.com)

Abstract. In this paper, the problem of Poiseuille flow with couple stresses effect in a fluid layer using the linear instability and nonlinear stability theories is analyzed. Also, the nonlinear stability eigenvalue problems for *x,z* and *y,z* disturbances are derived. The Chebyshev collocation method is adopted to arrive at the eigenvalue equation, which is then solved numerically, where the equivalent of the Orr-Sommerfeld eigenvalue problem is solved using the Chebyshev collocation method. The difficulties which arise in computing the spectrum of the Orr-Sommerfeld equation are discussed. The critical Reynolds number R_c, the critical wave number a_c, and the critical wave speed c_c are computed for wide ranges of the couple stresses coefficient M. It is found that the couple stresses coefficient M has great stabilizing effects on the fluid flow where the fluid flow becomes more unstable as M increases.

Keywords: Poiseuille flow, Couple stresses, Orr-Sommerfeld, Linear instability, Nonlinear stability.

1. Introduction

In this paper, we study the problem of Poiseuille flow. It involves an incompressible fluid under isothermal conditions, inside an infinite channel, which associates with a constant pressure gradient. In a laminar way, the fluid flows along this pressure gradient, resulting in a parabolic velocity profile which is independent of time. The actual difference from the previous work is that we add the effect of the couple stresses effect.

One of the main problems in fluid dynamics is the classical hydrodynamic problem of stability for Poiseuille flow in a channel, see for example Joseph [1], chapter 3, Straughan [2], chapter 8. These authors have shown that there are substantial problems in trying to improve or develop the nonlinear stability theory because there is a significant difference between the linear instability and the nonlinear energy thresholds. In addition, the associated eigenvalue problems to this class of flows are very difficult and need a very accurate numerical scheme, see for example [3, 4].

However, this area still attracts much interest in the literature of fluid dynamics. In [5], the nonlinear energy stability has been addressed. Poiseuille flows that time-dependent and time-periodic was analyzed in [6, 7]. The effect of slip boundary conditions has been studied in [8, 9]. Moreover, the Poiseuille flow problem of flow for a fluid overlying a porous medium has been introduced in [10, 11]. Also, the Poiseuille problem of flow in a channel with one fluid overlying another was studied in [4]. These articles include many other relevant references.

Earlier in this work, the theoretical and experimental results on the onset of thermal instability (Bénard convection) in a fluid layer under varying assumptions of hydrodynamics, underwent a detailed review, conducted by Chandrasekhar [12]. Such investigations of these kinds of fluids are important, bearing in mind the increasing importance of non-Newtonian fluids in technology and industries. Stokes [13] has put forward the theory of couple-stress fluids. Couple-stresses are present in significant magnitude in fluids with very large molecules. Applications of couple-stress fluids occur in connection with the study of the mechanism of synovial joint lubrication, currently being focussed upon by researchers.

Published online: February 10 2020

A human joint is a dynamically loaded bearing with articular cartilage as the bearing, and synovial fluid as the lubricant. The normal synovial fluid is clear or yellowish and is a non-Newtonian, viscous fluid. Because of the long chain of lauronic acid molecules found as additives in synovial fluid, Walicki and Walicka [14] modeled the fluid in question as couple-stress fluid in human joints. The issue of a couple-stress fluid and porous medium has also been investigated in [15-17]. Recently, in Harfash and Meftenb [18], the problem of convective movement of a reacting solute in a viscous incompressible fluid occupying a plane layer and subjected to a couple stresses effects have been studied. The thresholds for linear instability are found and compared to those derived by a global nonlinear energy stability analysis. However Harfash and Meftenb, in [19], have extended their work where they have studied the problem of double-diffusive convection in a reacting fluid with the effect of couple stresses. In [19], the density is assumed to have quadratic dependence on the temperature and a linear dependence on the concentration and Linear instability and nonlinear stability analyses were performed.

In the present article, the problem of Poiseuille flow of an incompressible couple stress fluid between parallel plates is studied using no-slip boundary conditions. Here, we consider a modification to the work in [20] by inserting the effect of couple stresses effect on the problem of Poiseuille flow in an infinite channel and discarding the effect of the magnetic field and we believe this problem is analyzed for the first time in this article. In order to provide a clear analysis of the problem of Orr-Sommerfeld, we discuss in this paper the instability of Poiseuille flow in the plane with the couple stresses effect. We then turn to the study of non-linear stability analysis of the problem. We also include our computational results for both cases.

2. Basic Equations

We suppose the Poiseuille flow with couple stresses type and occupies the spatial domain $\{(x,y)\in\mathbb{R}^2\}\times\{z\in(-L/2,L/2)\}\times\{t>0\}$, (schematically shown in Figs. 1 and 2), then, the governing equations are [13]:

$$\begin{gathered}\rho_0(v_{i,t}+v_j v_{i,j})=-p_{,i}+\mu\Delta v_i-\hat{\mu}\Delta^2 v_i,\\ v_{i,i}=0,\end{gathered}\tag{1}$$

where $v_i, p, \rho_0, \mu,$ and $\hat{\mu}$ denote the velocity field, pressure, density, dynamic viscosity coefficient, and couple stress viscosity coefficient, see [18, 19]. The equations (1) are conveniently non-dimensionalized scalings with the variables:

$$\mathbf{x}=L\mathbf{x}^*,\quad t=\frac{L}{V_0}t^*,\quad \mathbf{v}=V_0\mathbf{v}^*,\quad p=\frac{V_0\mu}{L}p^*,\quad M=\frac{\hat{\mu}}{\mu L^2},\ Re=\frac{\rho_0V_0L}{\mu}.$$

Now, from above non-dimensional, then the system (1) may be rewritten as:

$$\begin{gathered}Re(v_{i,t}+v_j v_{i,j})=-p_{,i}+\Delta v_i-M\Delta^2 v_i,\\ v_{i,i}=0,\end{gathered}\tag{2}$$

where Re is the Reynolds number and M is a non-dimensional couple stress viscosity coefficient. The above Equations are holding now on $\{(x,y)\in\mathbb{R}^2\}\times\{z\in(-1,1)\}\times\{t>0\}$, with the following no-slip boundary conditions, see [18, 19],

$$w_{yz}-v_{zz}=0\quad w_{xz}-u_{zz}=0,\ \text{and}\ v_i=0,\quad \text{on}\ \ z=-1,1.\tag{3}$$

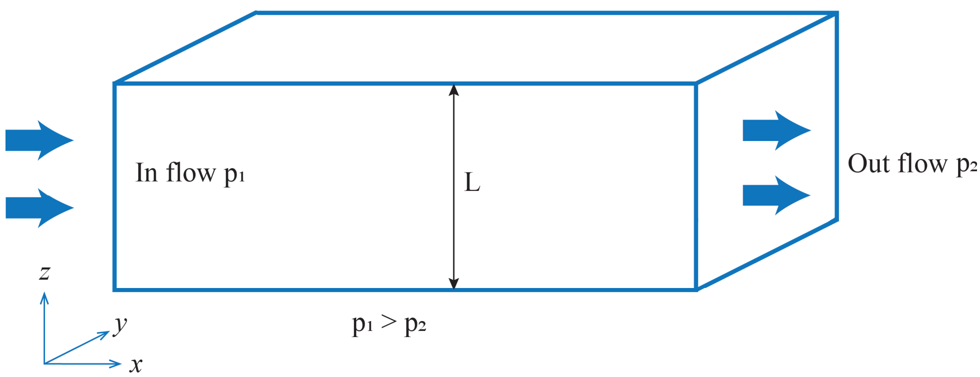

Fig. 1. A schematic of the physical domain.

$$w_{yz} - v_{zz} = 0, \quad w_{xz} - u_{zz} = 0 \quad \text{and} \quad v_i = 0 \quad \text{on} \quad z = 1$$

Fixed

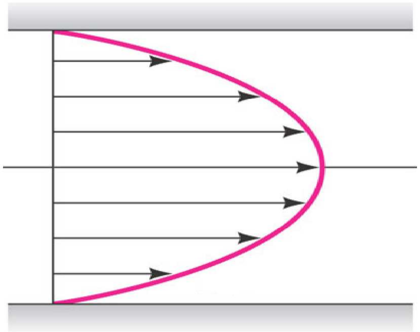

Fixed

$$w_{yz} - v_{zz} = 0, \quad w_{xz} - u_{zz} = 0 \quad \text{and} \quad v_i = 0 \quad \text{on} \quad z = -1$$

Fig. 2. Velocity profile.

The basic solution whose stability we are interested in is one where the fluid is driven along the channel in the x-direction by a constant pressure gradient of form

$$-\frac{\partial \overline{p}}{\partial x} = k^2 > 0,$$

where an over bar denotes the basic state, then,

$$\Delta \overline{v}_i - M\Delta^2 \overline{v}_i = -k^2,$$

the basic velocity field corresponding to this pressure gradient has form $\overline{v}_i = (U(z), 0, 0)$, such that

$$\Delta \overline{v}_i = (U''(z), 0, 0) \text{ and } \Delta^2 \overline{v}_i = (U^{(4)}(z), 0, 0).$$

Under these treatments, we have:

$$U'' - MU^{(4)} = -k^2,$$

where U'' and $U^{(4)}$ are the second and fourth derivatives of U, respectively. The boundary conditions are:

$$U(z) = 0, \quad z = \pm 1,$$

$$U''(z) = 0, \quad z = \pm 1,$$

By solving the above equation and applying the boundary conditions we arrive at:

$$U(z) = \frac{k^2 M}{\cosh(\frac{1}{\sqrt{M}})} \cosh(\frac{z}{\sqrt{M}}) - k^2 M + \frac{k^2}{2}(1 - z^2),$$

if in our non-dimensionalization we take $k^2 = 2$, then U reduce to:

$$U(z) = \frac{2M}{\cosh(\frac{1}{\sqrt{M}})} \cosh(\frac{z}{\sqrt{M}}) - 2M + 1 - z^2.$$

The perturbation forms are:

$$v_i = U + u_i \text{ and } p = \overline{p} + \pi.$$

Substituting the perturbed forms into equations (2), we obtain the perturbation equations:

$$\begin{gathered} Re(u_{i,t} + u_j u_{i,j} + u_j U_{i,j} + U_j u_{i,j}) = -\pi_{,i} + \Delta u_i - M\Delta^2 u_i, \\ u_{i,i} = 0. \end{gathered} \tag{4}$$

3. Linear Instability

To study linear instability, we ignore nonlinear terms in (4), then we obtain:

$$\begin{gathered} Re(u_{i,t}+u_jU_{i,j}+U_ju_{i,j})=-\pi_{,i}+\Delta u_i-M\Delta^2 u_i, \\ u_{i,i}=0, \end{gathered} \tag{5}$$

since $u_i=(u,v,w)$, then, the above equations can be written as the form:

$$\begin{gathered} Re(u_{,t}+wU'+Uu_{,1})=-\pi_{,1}+\Delta u-M\Delta^2 u, \\ Re(v_{,t}+Uv_{,1})=-\pi_{,2}+\Delta v-M\Delta^2 v, \\ Re(w_{,t}+Uw_{,1})=-\pi_{,3}+\Delta w-M\Delta^2 w, \\ u_x+v_y+w_z=0. \end{gathered} \tag{6}$$

6We consider a solution forms:

$$\begin{gathered} u=u(z)e^{i(\alpha x+\beta y-\alpha ct)}, \quad v=v(z)e^{i(\alpha x+\beta y-\alpha ct)}, \\ w=w(z)e^{i(\alpha x+\beta y-\alpha ct)}, \quad \pi=\pi(z)e^{i(\alpha x+\beta y-\alpha ct)}. \end{gathered} \tag{7}$$

Then, by substituting equations (7) in equations (6), yields:

$$\begin{gathered} i\alpha Re(U-c)u+RU'w=-i\alpha\pi+(D^2-\alpha^2-\beta^2)u-M(D^2-\alpha^2-\beta^2)^2u, \\ i\alpha Re(U-c)v=-i\beta\pi+(D^2-\alpha^2-\beta^2)v-M(D^2-\alpha^2-\beta^2)^2v, \\ i\alpha Re(U-c)w=-D\pi+(D^2-\alpha^2-\beta^2)w-M(D^2-\alpha^2-\beta^2)^2w, \\ i\alpha u+i\beta v+Dw=0. \end{gathered} \tag{8}$$

However, if we add $\alpha\times(7)_1$ to $\beta\times(7)_2$, and define:

$$a=\sqrt{\alpha^2+\beta^2},\ a\hat{u}=\alpha u+\beta v,\ \hat{w}=w,\ a\hat{R}e=\alpha Re \text{ and } a\hat{\pi}=\alpha\pi,$$

we obtain the system:

$$\begin{gathered} ia^2\hat{R}e(U-c)\hat{u}+a\hat{R}eU'\hat{w}=-ia^2\hat{\pi}+a(D^2-a^2)\hat{u}-aM(D^2-a^2)^2\hat{u}, \\ ia\hat{R}e(U-c)w=-D\hat{\pi}+(D^2-a^2)\hat{w}-M(D^2-a^2)^2\hat{w}, \\ ia\hat{u}+D\hat{w}=0, \end{gathered} \tag{9}$$

since $ia\hat{u}=-D\hat{w}$, then, equation (9), reduces to:

$$-a\hat{R}e(U-c)D\hat{w}+a\hat{R}eU'\hat{w}=-ia^2\hat{\pi}+i(D^2-a^2)D\hat{w}-iM(D^2-a^2)^2D\hat{w}. \tag{10}$$

Now, remove the pressure terms by performing $D\times(10)-ia^2\times(109)_2$, yields:

$$iaRe[(U-c)(D^2-a^2)-U']w=[(D^2-a^2)^2-M(D^2-a^2)^3]w. \tag{11}$$

where $z\in(-1,1)$, with the following boundary conditions:

$$W=DW=D^3W=0, \quad z=\pm1. \tag{12}$$

4. Nonlinear Theory

We use now the energy method to derive sufficient conditions to ensure the stability of the steady-state solution, i.e., we will find value Re_E so that the steady-state solution is stable $Re<Re_E$. Let $\|\cdot\|$ and are the norm and inner product on $L^2(\Omega)$, which have the form:

$$\langle f\,g\rangle=\int_\Omega f\,g\,dV, \ \ \|f\|=\sqrt{\langle f\,f\rangle} \quad f,g\in L^2(\Omega),$$

where $dV=dxdydz$ is a volume element and let $H^1(\Omega)$ be the complex Hilbert space of measurable functions which is defined on Ω such that for $f\in H^1(\Omega)$, we have:

$$\|f\|+\|f'\|<\infty.$$

We also define the subspace $\mathcal{H} \in [H^1(\Omega)]^3$, where for $\mathbf{u}=(u,v,w)\in\mathcal{H}$, then, $\nabla\cdot\mathbf{u}=0$, the components of $\mathbf{u}$ satisfying (3) and is periodic modulo Ω. Assuming $\mathbf{u}\in\mathcal{H}$, and let $E(t)$ is defined by:

$$E(t)=\frac{1}{2}\|\mathbf{u}\|^2$$

Now, we multiply the equation $(4)_1$ by u_i, yields:

$$\frac{dE}{dt}=\langle u_i(\frac{1}{Re}[-\pi_{,i}+\Delta u_i-M\Delta^2 u_i]-u_j u_{i,j}-u_j U_{i,j}-U_j u_{i,j})\rangle,$$

integrating by parts for each of these terms and applying $u_{i,i}=0$, we obtain:

$$\frac{dE}{dt}=-\frac{1}{2}\langle u_i u_j(U_{i,j}+U_{j,i})\rangle-\frac{1}{Re}(\|\nabla\mathbf{u}\|^2+M\|\Delta\mathbf{u}\|^2).$$

Now, let $F_{ij}=\frac{1}{2}(U_{i,j}+U_{j,i})$, thus, the energy equation can be reduced as:

$$\frac{dE}{dt}=\mathcal{I}-\frac{1}{Re}\mathcal{D}, \tag{13}$$

where

$$\mathcal{I}(\mathbf{u})=-\langle u_i u_j F_{ij}\rangle \quad \text{and} \quad \mathcal{D}(\mathbf{u})=\|\nabla\mathbf{u}\|^2+M\|\Delta\mathbf{u}\|^2,$$

if we define Re_E by:

$$\frac{1}{Re_E}=\max_{\mathbf{u}\in\mathcal{H}}\frac{\mathcal{I}}{\mathcal{D}}, \tag{14}$$

therefore, if $Re<Re_E$, we have:

$$\frac{dE}{dt}\le-\mathcal{D}(\frac{Re_E-Re}{ReRe_E}),$$

then with α being the constant in poincaré's inequality for $\mathbf{u}$, we have $\mathcal{D}\ge\alpha E$, hence:

$$\frac{dE}{dt}\le-\alpha(\frac{Re_E-Re}{ReRe_E})E(t)\Rightarrow E(t)\le e^{-\gamma t}E(0),$$

where $\gamma=\alpha(\frac{Re_E-Re}{ReRe_E})$. The decay of $E(t)$, and hence of $\mathbf{u}$ in an L^2 sense, follows from the above inequality. Now that global stability has been satisfied and then it remains to solve the variational problem (14). To solve the maximization problem we study the Euler Lagrange equations. For an arbitrary function $\mathbf{h}(\mathbf{u})\in\mathcal{H}$. Hence:

$$\frac{d}{d\varepsilon}\frac{\mathcal{I}(\mathbf{u}+\varepsilon\mathbf{h})}{\mathcal{D}(\mathbf{u}+\varepsilon\mathbf{h})}|_{\varepsilon=0}=\frac{1}{\mathcal{D}(\mathbf{u})}(\frac{d}{d\varepsilon}\mathcal{I}(\mathbf{u}+\varepsilon\mathbf{h})|_{\varepsilon=0}-\frac{1}{Re_E}\frac{d}{d\varepsilon}\mathcal{D}(\mathbf{u}+\varepsilon\mathbf{h})|_{\varepsilon=0})=0.$$

Now differentiate the $\mathcal{I}$ and $\mathcal{D}$ terms:

$$\begin{aligned}\frac{d}{d\varepsilon}\mathcal{I}(\mathbf{u}+\varepsilon\mathbf{h})|_{\varepsilon=0}&=-\frac{d}{d\varepsilon}\langle(u_i+\varepsilon h_i)(u_j+\varepsilon h_j)F_{ij}\rangle|_{\varepsilon=0}\\&=-\langle u_i h_j F_{ij}\rangle-\langle h_i u_j F_{ij}\rangle=-2\langle h_i u_j F_{ij}\rangle, \quad \text{such that } F_{ij} \text{ is symmetric}\end{aligned}$$

$$\frac{d}{d\varepsilon}\mathcal{D}(\mathbf{u}+\varepsilon\mathbf{h})|_{\varepsilon=0}=\frac{d}{d\varepsilon}(\|\nabla(\mathbf{u}+\varepsilon\mathbf{h})\|^2-\|\Delta(\mathbf{u}+\varepsilon\mathbf{h})\|^2)|_{\varepsilon=0}=2\langle\Delta u_i-M\Delta^2 u_i,h_i\rangle.$$

The condition $h_{i,i}=0$ can be included through the Lagrange multiplier $2\zeta(\mathbf{x})$, so that:

$$2\langle h_{i,i}\zeta\rangle=-2\langle h_i\zeta_{,i}\rangle.$$

Collecting together all terms in h_i, $\frac{I}{\mathcal{D}}$ is at an extremum provided that:

$$\langle(\Delta u_i - M\Delta^2 u_i - Re_E u_j F_{ij} + \zeta_{,i})h_i\rangle = 0.$$

As $\mathbf{h}$ was selected as an arbitrary function, and if we identify $\zeta(\mathbf{x})$ with the pressure π, the Euler-Lagrange equations have the following form:

$$\begin{gathered}\Delta u_i - M\Delta^2 u_i - Re_E u_j F_{ij} = -\pi_{,i}, \\ u_{i,i} = 0,\end{gathered} \tag{15}$$

therefore, our aim is to solve (15) which represents an eigenvalue problem in Re_E to find the smallest Reynolds number Re_E. By substituting $\overline{v}_i = (U(z),0,0)$, in (15), the above system has the following final form:

$$\begin{gathered}\Delta u - M\Delta^2 u - \frac{1}{2}RewU' = -\pi_{,x}, \\ \Delta v - M\Delta^2 v = -\pi_{,y}, \\ \Delta w - M\Delta^2 w - \frac{1}{2}ReuU' = -\pi_{,z}, \\ u_{,x} + v_{,y} + w_{,z} = 0.\end{gathered} \tag{16}$$

The Euler-Lagrange equations which are resulted in (16) are not in the form such that Squire's theorem can be applied. Therefore, here we examine the problems of $y-$ and $x-$ independent solutions.

4.1 Stability with respect to a *y*-independent perturbation

Let $\mathbf{u} = \mathbf{u}(x,z;t)$, then (15), reduces to:

$$\begin{gathered}\Delta u - M\Delta^2 u - \frac{1}{2}RewU' = -\pi_{,x}, \\ \Delta v - M\Delta^2 v = 0, \\ \Delta w - M\Delta^2 w - \frac{1}{2}ReuU' = -\pi_{,z}, \\ u_x + w_z = 0,\end{gathered} \tag{17}$$

where $\Delta = \frac{\partial^2}{\partial x^2} + \frac{\partial^2}{\partial z^2}$. It is clear that the v equation uncouples and the solution is $v = 0$. Thus, we can remove π by performing $\frac{\partial}{\partial z}\times(17)_1 - \frac{\partial}{\partial x}\times(1717)_3$, to have:

$$\Delta(u_{,z} - w_{,x}) - M\Delta^2(u_{,z} - w_{,x}) + \frac{1}{2}Re(u_{,x} - w_{,z})U' - \frac{1}{2}RewU'' = 0,$$

Differentiating above equation with respect to x and using $(17)_4$, to substituting $u_{,xx} = -w_{,zx}$ and $u_{,xz} = -w_{,zz}$ we arrive at the eigenvalue problem:

$$\Delta^2 w - M\Delta^3 w + Rew_{,xz}U' + \frac{1}{2}Rew_{,x}U'' = 0, \tag{18}$$

where $z \in (-1,1)$, we consider the solutions of equation (18) as the form $w = w(z)e^{iax}$ and substituting this form into (18), we obtain:

$$(D^2 - a^2)^2 w - M(D^2 - a^2)^3 w + iaRe(U'Dw + \frac{1}{2}wU'') = 0. \tag{19}$$

where w satisfies (12).

4.2 Stability with respect to a *x*-independent perturbation

Now, for stability with respect to $x-$ independent perturbation, we suppose that $\mathbf{u} = \mathbf{u}(y,z;t)$, then (15) reduces to:

$$\begin{gathered}\Delta u - M\Delta^2 u - \frac{1}{2} RewU' = 0,\\ \Delta v - M\Delta^2 v = -\pi_{,y},\\ \Delta w - M\Delta^2 w - \frac{1}{2} ReuU' = -\pi_{,z},\\ v_{,y} + w_{,z} = 0,\end{gathered} \tag{20}$$

we can eliminate π by performing $\frac{\partial}{\partial z}\times(20)_2 - \frac{\partial}{\partial y}\times(2020)_3$, yields:

$$\Delta(v_{,z} - w_{,y}) - M\Delta^2(v_{,z} - w_{,y}) + \frac{1}{2} Reu_{,y}U' = 0,$$

differentiating above equation with respect to y and using $(20)_4$ to substituting $v_{,yy} = -w_{,zy}$ and $v_{,yz} = -w_{,zz}$, yields:

$$\Delta^2 w - M\Delta^3 w - \frac{1}{2} Reu_{,yy}U' = 0. \tag{21}$$

Now consider the solutions of equation (21) as the form $u = u(z)e^{iay}$ and $w = w(z)e^{iay}$ and substituting this form into (21) and (20),:

$$\begin{gathered}2(D^2 - a^2)^2 w - 2M(D^2 - a^2)^3 w + a^2 ReuU' = 0,\\ 2(D^2 - a^2)u - 2M(D^2 - a^2)^2 u - RewU' = 0\end{gathered} \tag{22}$$

5. Numerical Techniques

Since solving equation (11) is a very difficult numerical problem for finding the eigenvalues, we will utilize a very accurate numerical method, which is the Chebyshev collocation method. The eigenvalue systems of linear instability and nonlinear stability theories have been solved using the Chebyshev collocation method, for more details see [25-33]. As these texts point out that the advantage in using the Chebyshev collection method is that it can achieve the required accuracy using a small number of polynomials, allowing the achievement of highly accurate results with short run time. Moreover, this method has the highest accuracy between the numerical methods and requires a smaller number of polynomials to achieve excellent accuracy and convergence. Also, the above texts note that the Chebyshev collection method is one of the best choices in solving the hydrodynamic stability problems as it is a flexible method and it can give very accurate results.

Firstly, the functions $A = Dw$ and $B = D^3 w$ are introduced, then equation (11) can be written in the following form:

$$\begin{aligned}&Dw - A = 0,\\ &D^2 A - B = 0,\\ &(a^4 + a^6 M + ia^3 ReU + iaReU'')w - (2a^2 + 3a^4 M + iaReU)DA\\ &+(D - MD^3 + 3a^2 MD)B = ia^3 cRew - iacReDA.\end{aligned} \tag{23}$$

The boundary conditions (12) have the form:

$$A = B = w = 0, \quad z = \pm 1, \tag{24}$$

To use the Chebyshev collocation method, we write solutions for the equations (23) and (24) as the sum of a limited number of Chebyshev polynomials, so these solutions take the following forms:

$$w = \sum_{n=0}^{N} w_n T_n(z), \qquad A = \sum_{n=0}^{N} A_n T_n(z), \qquad B = \sum_{n=0}^{N} B_n T_n(z). \tag{25}$$

where $T_n(z)$ are the Chebyshev polynomials of the first kind, see [3], which is defined by:

$$T_0(z) = 1, \;\; T_1(z) = z$$

$$T_{n+1}(z) - 2zT_n(z) + T_{n-1}(z) = 0, \;\; -1 \le z \le 1$$

or

$$T_n(z) = \cos(n \arccos(z)), \;\; -1 \le z \le 1.$$

The expression (25) is employed in equations (23) and (24) and then the resulting equations are computed at Gauss-Lobatto points y_i which are defined by $y_i = \cos(\pi i / [N-3]), i = 0,\ldots,N-2$. This gives $3N-3$ equations for $3N+3$ unknowns $w_0,\ldots,w_N, A_0,\ldots,A_N, B_0,\ldots,B_N$. The remaining 6 equations are furnished by the boundary conditions (24) which becomes:

$$\begin{aligned} &BC_1:\sum_{n=0}^{N} w_n = 0, \qquad BC_2:\sum_{n=0}^{N}(-1)^n w_n = 0, \qquad BC_3:\sum_{n=0}^{N} A_n = 0,\\ &BC_4:\sum_{n=0}^{N}(-1)^n A_n = 0, \qquad BC_5:\sum_{n=0}^{N} B_n = 0, \qquad BC_6:\sum_{n=0}^{N}(-1)^n B_n = 0, \end{aligned} \tag{26}$$

then approximated boundary conditions (26) are added as rows to the generated matrices to yield a $(3N+3)\times(3N+3)$ eigenvalue matrix. Thus, we have the eigenvalue system:

$$\begin{pmatrix} D & -I & O \\ BC_1 & 0,\ldots,0 & 0,\ldots,0 \\ BC_2 & 0,\ldots,0 & 0,\ldots,0 \\ O & D^2 & -I \\ 0,\ldots,0 & BC_3 & 0,\ldots,0 \\ 0,\ldots,0 & BC_4 & 0,\ldots,0 \\ A_1 & A_2 & A_3 \\ 0,\ldots,0 & 0,\ldots,0 & BC_5 \\ 0,\ldots,0 & 0,\ldots,0 & BC_6 \end{pmatrix} X = c \begin{pmatrix} O & O & O \\ 0,\ldots,0 & 0,\ldots,0 & 0,\ldots,0 \\ O & O & O \\ 0,\ldots,0 & 0,\ldots,0 & 0,\ldots,0 \\ 0,\ldots,0 & 0,\ldots,0 & 0,\ldots,0 \\ ia^3 ReI & -iaReD & O \\ 0,\ldots,0 & 0,\ldots,0 & 0,\ldots,0 \\ 0,\ldots,0 & 0,\ldots,0 & 0,\ldots,0 \end{pmatrix} X, \tag{27}$$

where $X = (w_0,\ldots,w_N, A_0,\ldots,A_N, B_0,\ldots,B_N)$, O is the zeros matrix,

$$A_1(n_1,n_2) = (a^4 + a^6 M + iaReU''(y_{n_1}) + ia^3 ReU(y_{n_1}))I(n_1,n_2),$$

$$A_2(n_1,n_2) = -(2a^2 + 3a^4 M + iaReU(y_{n_1}))D(n_1,n_2)$$

$$A_3(n_1,n_2) = (1+3a^2 M)D(n_1,n_2) - MD^3(n_1,n_2)$$

$$I(n_1,n_2) = T_{n_2}(y_{n_1}), \quad D(n_1,n_2) = T'_{n_2}(y_{n_1}), \quad D^2(n_1,n_2) = T''_{n_2}(y_{n_1}), \quad D^3(n_1,n_2) = T'''_{n_2}(y_{n_1}),$$

$$n_1 = 0,\ldots,N-2, \quad n_2 = 0,\ldots,N.$$

The above system has been solved using the QZ algorithm. For a perturbation u,v,w,π dependent on x,z, we implement the Chebyshev collocation method to the eigenvalue problem (29) to obtain the linear system:

$$\begin{pmatrix} D & -I & O \\ BC_1 & 0,\ldots,0 & 0,\ldots,0 \\ BC_2 & 0,\ldots,0 & 0,\ldots,0 \\ O & D^2 & -I \\ 0,\ldots,0 & BC_3 & 0,\ldots,0 \\ 0,\ldots,0 & BC_4 & 0,\ldots,0 \\ A_1 & A_2 & A_3 \\ 0,\ldots,0 & 0,\ldots,0 & BC_5 \\ 0,\ldots,0 & 0,\ldots,0 & BC_6 \end{pmatrix} X = Re \begin{pmatrix} O & O & O \\ 0,\ldots,0 & 0,\ldots,0 & 0,\ldots,0 \\ O & O & O \\ 0,\ldots,0 & 0,\ldots,0 & 0,\ldots,0 \\ 0,\ldots,0 & 0,\ldots,0 & 0,\ldots,0 \\ A4 & A5 & O \\ 0,\ldots,0 & 0,\ldots,0 & 0,\ldots,0 \\ 0,\ldots,0 & 0,\ldots,0 & 0,\ldots,0 \end{pmatrix} X, \tag{28}$$

$$(D^2 - a^2)^2 w - M(D^2 - a^2)^3 w + iaRe(U'Dw + \frac{1}{2}wU'') = 0. \tag{29}$$

where $X = (w_0,\ldots,w_N, A_0,\ldots,A_N, B_0,\ldots,B_N)$, $A_5(n_1,n_2) = \frac{1}{2} iaU''(y_{n_1})I(n_1,n_2)$, $A_5(n_1,n_2) = iaU'(y_{n_1})I(n_1,n_2)$, and $n_1 = 0,\ldots,N-2$, $n_2 = 0,\ldots,N$. However, for the eigenvalue system for $x-$ independent solutions (22), the Chebyshev collocation method yields the eigenvalue system of the form:

$$\hat{A}X = Re\hat{B}, \tag{30}$$

where

$$\hat{A} = \begin{pmatrix} D & -I & O & O & O \\ BC_1 & 0,\ldots,0 & 0,\ldots,0 & 0,\ldots,0 & 0,\ldots,0 \\ BC_2 & 0,\ldots,0 & 0,\ldots,0 & 0,\ldots,0 & 0,\ldots,0 \\ O & D^2 & -I & O & O \\ 0,\ldots,0 & BC_3 & 0,\ldots,0 & 0,\ldots,0 & 0,\ldots,0 \\ 0,\ldots,0 & BC_4 & 0,\ldots,0 & 0,\ldots,0 & 0,\ldots,0 \\ A_1 & A_2 & A_3 & O & O \\ 0,\ldots,0 & 0,\ldots,0 & BC_5 & 0,\ldots,0 & 0,\ldots,0 \\ 0,\ldots,0 & 0,\ldots,0 & BC_6 & 0,\ldots,0 & 0,\ldots,0 \\ O & O & O & D^2 & -I \\ 0,\ldots,0 & 0,\ldots,0 & 0,\ldots,0 & BC_7 & 0,\ldots,0 \\ 0,\ldots,0 & 0,\ldots,0 & 0,\ldots,0 & BC_8 & 0,\ldots,0 \\ O & O & O & A6 & A7 \\ 0,\ldots,0 & 0,\ldots,0 & 0,\ldots,0 & 0,\ldots,0 & BC_9 \\ 0,\ldots,0 & 0,\ldots,0 & 0,\ldots,0 & 0,\ldots,0 & BC_{10} \end{pmatrix}, \tag{31}$$

$$\hat{B} = \begin{pmatrix} O & O & O & O & O \\ 0,\ldots,0 & 0,\ldots,0 & 0,\ldots,0 & 0,\ldots,0 & 0,\ldots,0 \\ O & O & O & O & O \\ 0,\ldots,0 & 0,\ldots,0 & 0,\ldots,0 & 0,\ldots,0 & 0,\ldots,0 \\ 0,\ldots,0 & 0,\ldots,0 & 0,\ldots,0 & 0,\ldots,0 & 0,\ldots,0 \\ O & O & O & A_8 & O \\ 0,\ldots,0 & 0,\ldots,0 & 0,\ldots,0 & 0,\ldots,0 & 0,\ldots,0 \\ 0,\ldots,0 & 0,\ldots,0 & 0,\ldots,0 & 0,\ldots,0 & 0,\ldots,0 \\ O & O & O & O & O \\ 0,\ldots,0 & 0,\ldots,0 & 0,\ldots,0 & 0,\ldots,0 & 0,\ldots,0 \\ 0,\ldots,0 & 0,\ldots,0 & 0,\ldots,0 & 0,\ldots,0 & 0,\ldots,0 \\ A_9 & O & O & O & O \\ 0,\ldots,0 & 0,\ldots,0 & 0,\ldots,0 & 0,\ldots,0 & 0,\ldots,0 \\ 0,\ldots,0 & 0,\ldots,0 & 0,\ldots,0 & 0,\ldots,0 & 0,\ldots,0 \end{pmatrix}, \tag{32}$$

$$X = (w_0,\ldots,w_N, A_0,\ldots,A_N, B_0,\ldots,B_N, u_0,\ldots,u_N, C_0,\ldots,C_N),$$

$$C = D^2u, \quad BC_7 : \sum_{n=0}^{N} u_n = 0, \quad BC_8 : \sum_{n=0}^{N}(-1)^n u_n = 0, \quad BC_9 : \sum_{n=0}^{N} C_n = 0, \quad BC_{10} : \sum_{n=0}^{N}(-1)^n C_n = 0, \tag{33}$$

$$A_6(n_1,n_2) = -(a^2 + Ma^4)I(n_1,n_2), \qquad A_7(n_1,n_2) = (1+2a^2M)I(n_1,n_2) - MD^2(n_1,n_2),$$
$$A_8(n_1,n_2) = -\frac{1}{2}a^2U'(y_{n_1})I(n_1,n_2), \qquad A_9(n_1,n_2) = \frac{1}{2}U'(y_{n_1})I(n_1,n_2), \tag{34}$$
$$\text{and} \quad n_1 = 0,\ldots,N-2, \quad n_2 = 0,\ldots,N.$$

For a given a and M, then we use QZ algorithm of Matlab routines to solve the eigenvalue system, and next, we iterate this procedure over choices of a, tracking the smallest eigenvalue until we have found the critical Reynolds number which we denote by Re_E.

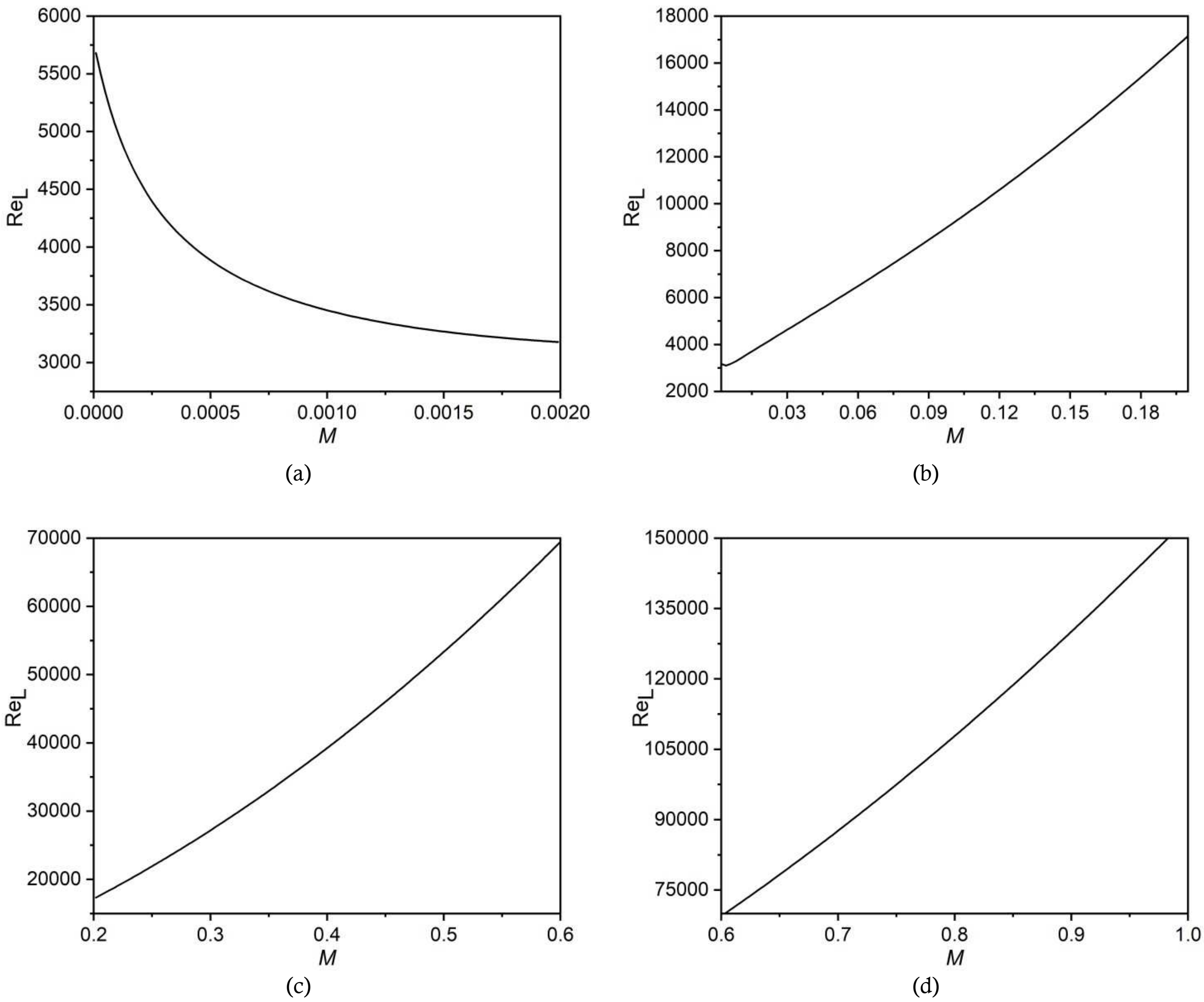

Fig. 3. Critical Reynolds number Re_L against M.

6. Numerical Results

In Table 1, the numerical results for the critical value Re are displayed for linear instability and nonlinear energy stability theory. It is very clear that there is a big difference between linear and nonlinear thresholds. This difference shows that there is a potential region of subcritical instabilities area may arise.

The critical Reynolds numbers are shown in Fig. 3, where instability curves were plotted as a function of the couple stresses coefficient M. The curves can be explained as follows. For instance, when $0 < M \leq 0.002$, the instability curve has been shown in Fig. 3 (a). For Re values below this curve, the solution is linearly stable, and the imaginary part of all eigenvalues is negative, i.e. $c_i < 0$. For Re values that are above this curve, then we should have at least one eigenvalue which has the imaginary part is positive, i.e. $c_i > 0$ and the solution grows exponentially and is unstable. A similar explanation holds for the other Figures. We note that as M increases, the critical Reynolds number increases substantially. This shows the strong stabilizing effect of the couple stresses coefficient M. Thus, the increasing M value leads to strongly increase the threshold at which instability commences.

The critical values of c_r as a function of M have shown in Fig. 4. As M vary, these values refer to how oscillatory the solution is in time at the start of instability.

The critical wavenumber curves against M are displayed in Fig. 5, where M varying over the range $M = 0$ to $M = 1$. These curves are explained as those for Re_L, where above these curve we have instability region, while the region below these curves are linearly stable. We also note that the values of critical wavenumber increase with increasing the values M and this means that the periodic cells of the w become smaller in the x and y directions.

In Fig. 6, the eigenvalues spectrum are introduced and we have found that are similar to that found for Poiseuille flow in a porous medium with no-slip boundary conditions in [21] and slip boundary conditions in [9]. The eigenvalues displaying a Y shape in the (c_r, c_i) diagram. As M increase, the eigenvalues at the intersection of the three lines in the Y become more numerically unstable, and this effect becomes clearer when the value of M is increased.

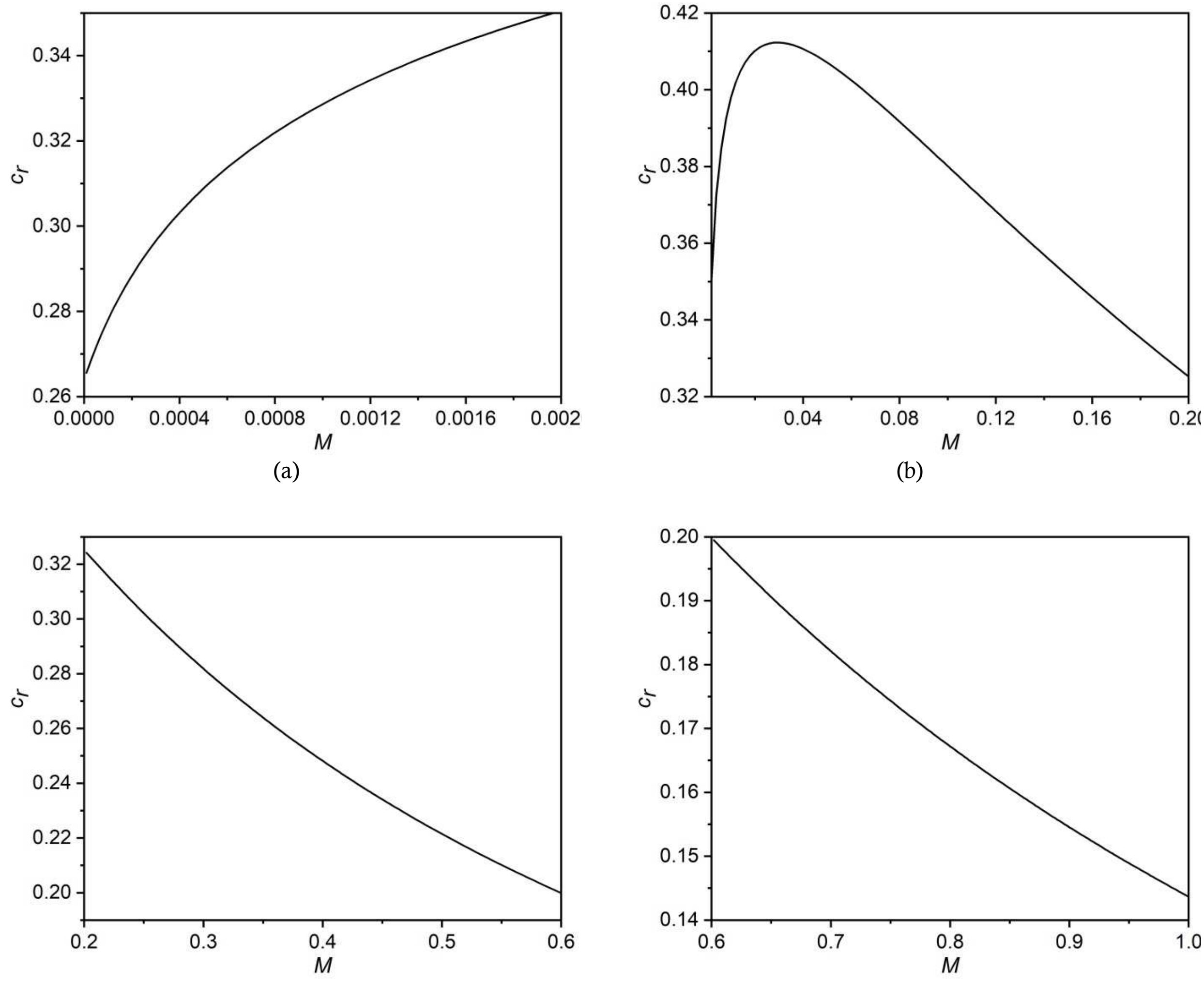

Fig. 4. Critical value of c_r against M.

The spectrum of (23) and (24) acting very like to that of the Orr-Sommerfeld problem for classical Poiseuille flow. For example, for higher Reynolds numbers we witnessed mode crossing of eigenvalues. For instance, for $M = 0.5$, the first and second eigenvalues interchange places for Re between 55500 and 55502, respectively, with the previous first eigenvalue moving down the list as Re increases. This behavior is very like to that noted in [3]. Also, the spectrum is highly sensitive and the number of polynomials that are used in the numerical approximation should be carefully selected, and in the arithmetical precision used in the calculation (those shown here are all $s64$ bit arithmetic). The spectrum for $M = 0.3, a = 5$ and $Re = 10^6$ are shown in Fig. 5, respectively, for different values of N. Since U is an even function of z, then, the proper solution of the eigenvalue system (23) and (24) locates in two unincorporated groups for even and odd solutions.

An interesting question for this problem can appear which relates to the accuracy of the expected results when comparing the results of linear instability and nonlinear stability theories. Therefore, this problem is one of the most difficult flow problems even in a clear fluid with slip and no-slip boundary conditions, see e.g. [2, 9]. The results of the linear instability guarantee that the solution is not stable for the Rayleigh number which exceeds the linear threshold. However, it does not guarantee stability when the Rayleigh number is below this. The nonlinear energy stability thresholds of nonlinear show the stability only where the solution is stable if the Rayleigh number is below this threshold, however, they say nothing about instability. Therefore, in this paper, we compute the nonlinear energy stability thresholds for our problem, just as in porous medium with the conditions of no-slip boundary by Hill & Straughan [11], and as was done for a clear fluid with slip boundary conditions by Webber & Straughan [8]; the work which are also carefully reported in chapter 3 of Webber [22]. For the current problem, the nonlinear energy stability thresholds which confirm the area of the stability of the solution are well below those of linear theory. This is one field in which the theory of nonlinear stability is not useful, and from these not unknown scenarios in other fields of mechanically fluid, see. Straughan [23], where there is a big difference discrepancy between the linear instability and the nonlinear stability thresholds. This shows that there is a potential region of subcritical instabilities area may arise. A fully three-dimensional simulation for some problems [24-29] shows that there is a region of subcritical instability below the linear instability threshold, but well above the nonlinear energy stability boundary.

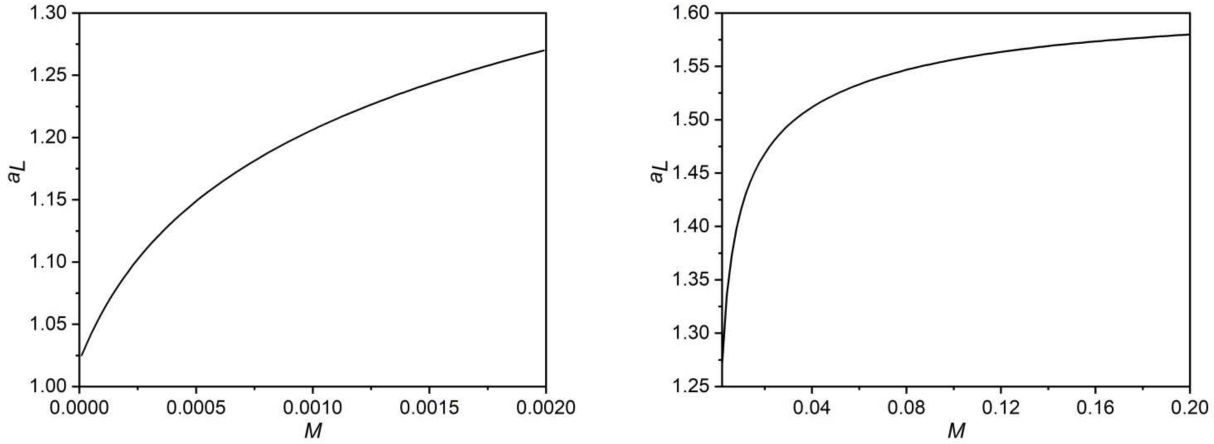

(a) (b)

Fig. 5. Critical wavenumber a_L against M.

Table 1. Critical Reynolds number Re, wavenumber a and wave speed c_r against couple stresses number M.

M	Re_L	a_L	c_r	Re_E^{xz}	a_E^{xz}	Re_E^{yz}	a_E^{yz}
0.1	9151.467	1.556	0.38	365.39	1.862	140.967	1.72
0.2	17150.775	1.58	0.325	720.667	1.827	259.884	1.661
0.3	27174.461	1.589	0.282	1167.031	1.814	408.652	1.634
0.4	39232.453	1.595	0.248	1705.333	1.806	587.354	1.62
0.5	53325.548	1.598	0.221	2335.794	1.796	796.01	1.61
0.6	69454.032	1.6	0.2	3058.484	1.797	1034.628	1.603
0.7	87617.993	1.602	0.182	3873.448	1.79	1303.209	1.599
0.8	107817.56	1.602	0.167	4780.716	1.788	1601.757	1.595
0.9	130052.74	1.603	0.155	5780.265	1.787	1930.271	1.592
1	154323.72	1.604	0.144	6872.148	1.786	2288.752	1.59

Table 2. Comparison between the critical Reynolds numbers (minimized over the wavenumber) of Takashima [20], Hill & Straughan [11], Harfash [34], and this paper for $M = 0$.

Methods	R_{crit}
Takashima [20], Chebyshev collocation by imposing BCs.	5772.2218
Hill & Straughan [11] Chebyshev-Tau method	5772
Harfash [34] Chebyshev collocation method with even Polynomials	5772.22198
Harfash [34], Finite element	5771.920022
The present work	5772.222169

Finally, in order to validate our numerical method, we compare the critical Reynolds numbers of Takashima [20], Hill & Straughan [11], Harfash [34], and this paper for $M = 0$. In the other studies M has different definitions but $M = 0$ the equivalent of the Orr-Sommerfeld eigenvalue problem becomes identical and therefore the critical Reynolds numbers should also identical. It is noted that there is very little variation with the critical Reynolds numbers observed by the other studies, as is shown in Table 2. This confirms the high accuracy of the numerical method which is used in this paper.

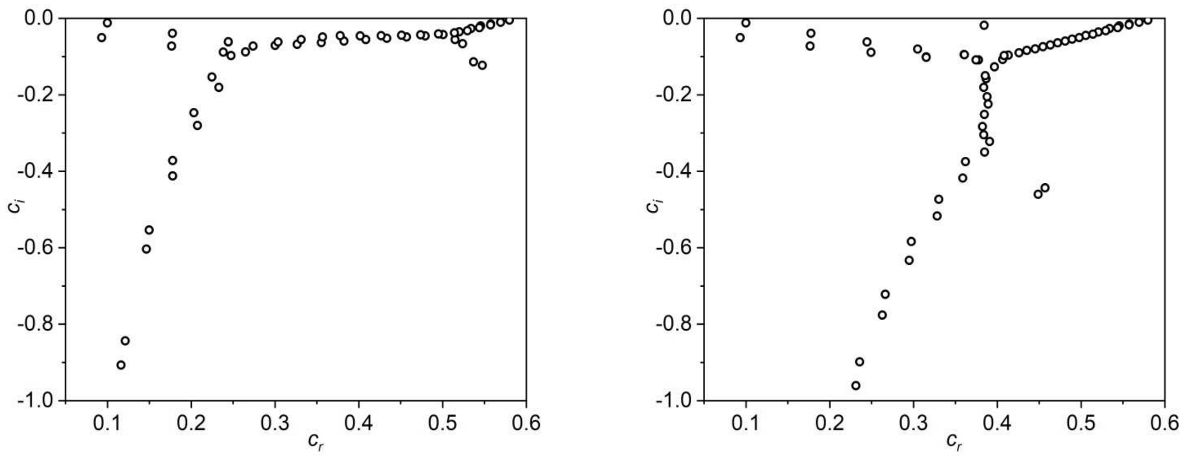

(a) $N = 75$ (b) $N = 100$

Fig. 6. Spectral of growth rate $c = c_r + ic_i$ at $M = 0.3$.

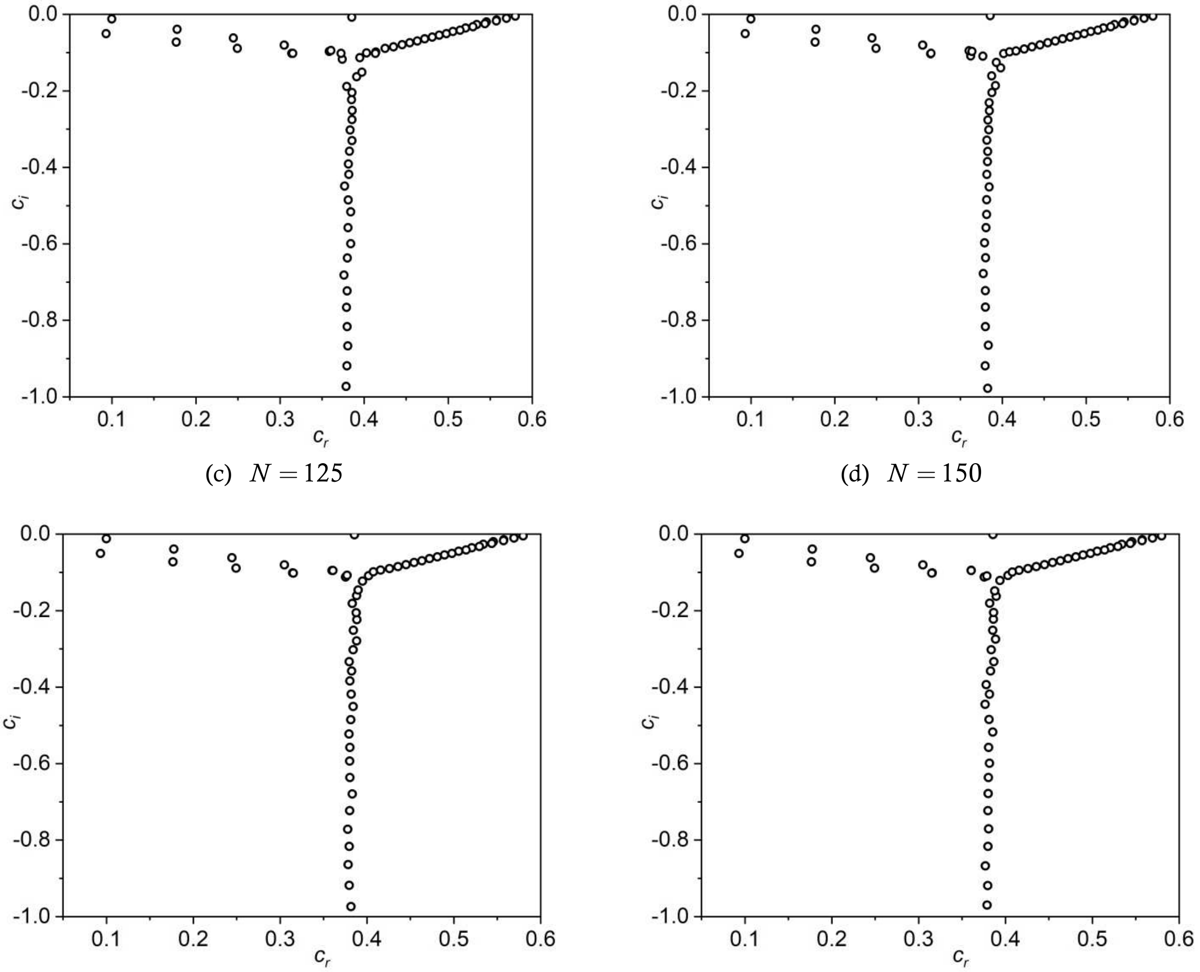

(c) $N = 125$ (d) $N = 150$

(e) $N = 175$ (f) $N = 200$

Fig. 6. Continued.

7. Conclusions

A linear instability analysis and nonlinear stability analyses for Poiseuille under the effect of couple stresses were presented. In deriving the equations governing the stability, a simplification was made using the fact that and the flow was driven by a constant pressure gradient in the direction. Using modified Squire's transformations, it was established the nonlinear stability for and disturbances. Also, the Chebyshev collocation method with the algorithm was used for solving the stability equations to find the eigenvalues. The secant and the golden section search were also utilized to compute the critical values. The critical numerical values of Reynolds number, wave number, and wave speed were computed for several selected values of the couple stress coefficient. For Poiseuille flow, we can conclude that the couple stresses have a stabilizing effect on the flow where as increases, the critical Reynolds number increases to stabilize the flow. The results of the present study confirm the impact of the non-Newtonian effects on the flow instability. Hence, further works can be provided to study the linear instability and nonlinear stability behaviors of new fluids such as suspension and slurries of nano-encapsulated phase change materials, see for examples [35-39].

Author Contributions

The authors conceived the mathematical model, proved the mathematical results and wrote the paper together. The authors gave their final approval for publication.

Acknowledgments

This work was supported by the Iraqi Ministry of Higher Education and Scientific Research. We should like to thank an editor and anonymous referee for suggestions that have led to improvements in the manuscript.

Conflict of Interest

The authors declared no potential conflicts of interest with respect to the research, authorship, and publication of this article.

Funding

The authors received no financial support for the research, authorship, and publication of this article.

References

[1] Joseph, D.D., *Stability of fluid motions I*. Springer, New York 1976.
[2] Straughan, B., *Explosive instabilities in mechanics*, Springer, Heidelberg, 1998.
[3] Dongarra, J.J., Straughan, B., Walker, D.W., Chebyshev tau-QZ algorithm methods for calculating spectra of hydrodynamic stability problems, *Applied Numerical Mathematics*, 22(4), 1996, 399-434
[4] Yecko, P., Disturbance growth in two-fluid channel flow: The role of capillarity, *International Journal of Multiphase Flow*, 34(3), 2008, 272-282.
[5] Kaiser, R., Mulone, G., A note on nonlinear stability of plane parallel shear flows, *Journal of Mathematical Analysis and Applications*, 302(2), 2005, 543-556.
[6] Galdi, G.P., Robertson, A.M., The relation between flow rate and axial pressure gradient for time-periodic Poiseuille flow in a pipe, *Journal of Mathematical Fluid Mechanics*, 7(2), 2005, S215-S223.
[7] Galdi, G.P., Pileckas, K., Silvestre, A.L., On the unsteady Poiseuille flow in a pipe, *Zeitschrift für angewandte Mathematik und Physik*, 58(6), 2007, 994-1007.
[8] Webber, M., Straughan, B., Stability of pressure-driven flow in a microchannel, *Rendiconti del Circolo Matematico di Palermo: serie II*, 78(2), 2006, 343-357.
[9] Straughan, B., Harfash, A.J., Instability in Poiseuille flow in a porous medium with slip boundary conditions, *Microfluidics and Nanofluidics*, 15(1), 2013, 109-115.
[10] Chang, M.H., Chen, F., Straughan, B., Instability of Poiseuille flow in a fluid overlying a porous layer, *Journal of Fluid Mechanics*, 564, 2006, 287-303.
[11] Hill, A.A., Straughan, B., Poiseuille flow in a fluid overlying a porous medium, *Journal of Fluid Mechanics*, 603, 2008, 137-149.
[12] Chandrasekhar, S., *Hydrodynamic and hydromagnetic stability*, Dover, New York, 1981.
[13] Stokes, V.K., Couple stresses in fluids, *The Physics of Fluids*, 9(9), 1966, 1709-1715.
[14] Walicki, E., Walicka, A., Interia effect in the squeeze film of a couple-stress fluid in biological bearings, *Applied Mechanics and Engineering*, 4(2), 1999, 363-373.
[15] Gaikwad, S.N., Kouser, S., Double diffusive convection in a couple stress fluid-saturated porous layer with internal heat source, *International Journal of Heat and Mass Transfer*, 78, 2014, 1254-1264.
[16] Devi, R., Mahajan, A., Global stability for thermal convection in a couple-stress fluid, *International Communications in Heat and Mass Transfer*, 38(7), 2011, 938-942.
[17] Malashetty, M.S., Kollur, P., The onset of double-diffusive convection in a couple of stress fluid-saturated anisotropic porous layer, *Transport in Porous Media*, 86(2), 2011, 435-459.
[18] Harfash, A.J., Meftenb, G.A., Couple stresses effect on linear instability and nonlinear stability of convection in a reacting fluid, *Chaos, Solitons, and Fractals*, 107, 2018, 18-25
[19] Harfash, A.J., Meftenb, G.A., Couple stresses effect on instability and nonlinear stability in a double-diffusive convection, *Applied Mathematics, and Computation*, 341, 2019, 301–320.
[20] Takashima, M., The stability of the modified plane Poiseuille flow in the presence of a transverse magnetic field, *Fluid Dynamics Research*, 17(6), 1996, 293-310.
[21] Hill, A.A., Straughan, B., *Stability of Poiseuille flow in a porous medium*, In R. Rannacher and A. Sequeira, editors, Advances in Mathematical Fluid Mechanics, Springer, Heidelberg, 2010.
[22] Webber, M., *Instability of fluid flows, including boundary slip*, Ph.D. thesis, Durham University, 2007.
[23] Straughan, B., Triply resonant penetrative convection, *Proceedings of the Royal Society A: Mathematical, Physical and Engineering Sciences*, 468(2148), 2012, 3804-3823.
[24] Harfash, A.J., Three-dimensional simulation of radiation induced convection, *Applied Mathematics and Computation*, 227, 2014, 92-101.
[25] Harfash, A.J., Three-dimensional simulations for convection induced by the selective absorption of radiation for the Brinkman model, *Meccanica*, 51(3), 2016, 501-515.
[26] Harfash, A.J., Alshara, A.K., On the stationary and oscillatory modes of triply resonant penetrative convection, *International Journal of Numerical Methods for Heat and Fluid Flow*, 26(5), 2016, 1391 - 1415.
[27] Harfash, A.J., Resonant penetrative convection in porous media with an internal heat source/sink effect, *Applied Mathematics and Computation*, 281, 2016, 323-342.
[28] Harfash, A.J., Stability analysis for penetrative convection in a fluid layer with throughflow, *International Journal of Modern Physics C*, 27(9), 2016, 1650101.
[29] Harfash, A.J., Nonhomogeneous porosity and thermal diffusivity effects on a double-diffusive convection in anisotropic porous media, *International Journal of Nonlinear Sciences and Numerical Simulation*, 17(5), 2016, 205-220.
[30] Harfash, A.J., Nashmi, F. K., Triply resonant double-diffusive convection in a fluid layer, *Mathematical Modelling and Analysis,* 22, 2017, 809-826.
[31] Harfash, A.J., H. A. Challoob, Slip boundary conditions and through flow effects on double-diffusive convection in

internally heated heterogeneous Brinkman porous media, *Chinese Journal of Physics*, 56, 2018, 10-22.
[32] Hameed, A.A., Harfash, A.J., Unconditional nonlinear stability for double-diffusive convection in a porous medium with temperature-dependent viscosity and density, *Heat Transfer-Asian Research*, 48, 2019, 2948-2973.
[33] Challoob, H.A., Mathkhor, A.J., Harfash, A.J., Slip boundary condition effect on double-diffusive convection in a porous medium: Brinkman Model, *Heat Transfer-Asian Research*, 49, 2020, 258-268.
[34] Harfash, A.J., Numerical methods for solving some hydrodynamic stability problems, *International Journal of Applied and Computational Mathematics*, 1, 2015, 293–326.
[35] Ghalambaz, M., Grosan, T., Pop, I., Mixed convection boundary layer flow and heat transfer over a vertical plate embedded in a porous medium filled with a suspension of nano-encapsulated phase change materials, *Journal of Molecular Liquids*, 293, 2019, 111432.
[36] Ghalambaz, M., Chamkha, A.J., Wen, D., Natural convective flow and heat transfer of Nano-Encapsulated Phase Change Materials (NEPCMs) in a cavity, *International Journal of Heat and Mass Transfer*, 138, 2019, 738-749
[37] Mehryan, S. A. M., Izadpanahi, E., Ghalambaz, M., Chamkha, A.J., Mixed convection flow caused by an oscillating cylinder in a square cavity filled with Cu–Al O/water hybrid nanofluid, *Journal of Thermal Analysis and Calorimetry*, 137, 2019, 965-982.
[38] Hajjar, A., Mehryan, S.A.M., Ghalambaz, M., Time periodic natural convection heat transfer in a nano-encapsulated phase-change suspension, *International Journal of Mechanical Sciences*, 166, 2020, 105243.
[39] Ghalambaz, M., Doostani, A., Izadpanahi, E., Chamkha, A.J., Conjugate natural convection flow of Ag–MgO/water hybrid nanofluid in a square cavity, *Journal of Thermal Analysis and Calorimetry*, 2019, doi:10.1007/s10973-019-08617-7.

ORCID iD

Akil J. Harfash https://orcid.org/0000-0002-3738-4242
Ghazi A. Meften https://orcid.org/0000-0003-0900-9303

How to cite this article: Harfash A.J., Meften J.A. Poiseuille Flow with Couple Stresses Effect and No-slip Boundary Conditions, *J. Appl. Comput. Mech.*, 6(SI), 2020, 1069–1083. https://doi.org/10.22055/JACM.2019.31964.1946